Effects of Solubilized Homopolymer on Lamellar Diblock Copolymer Structures

J. D. Vavasour and M. D. Whitmore*

Department of Physics and Physical Oceanography, Memorial University of Newfoundland, St. John's, NF, Canada, A1B 3X7

Received December 7, 2000; Revised Manuscript Received February 20, 2001

ABSTRACT: This paper examines binary blends of homopolymer with diblock copolymer, using numerical self-consistent field (NSCF) theory. On the basis of the general formalism, we identify the minimum number of characteristics of a blend needed to predict its equilibrium morphology and domain sizes. We then specialize to the case of A homopolymer added to A-*b*-B copolymer and carry out a series of NSCF calculations of the effects of solubilized homopolymer and its distribution throughout each domain. We present a detailed analysis of when the added homopolymer induces an increase or decrease in the domain thickness, compare strong and weak segregation behavior, identify the dominant controlling characteristics and the underlying physics, and make quantitative comparison with experiment. Many of the results are captured in a simple equation. We also suggest a procedure for determining χ parameters.

1. Introduction

There has been a great deal of experimental and theoretical work on the equilibrium phase behavior and detailed structure of block copolymers. The behavior exhibits many features that are common to different species and architectures, with relatively minor variations among different systems. Some of the extensive literature is cited in refs 1 and 2.

There is now good agreement between the observed microphase behavior and that predicted by numerical self-consistent field (NSCF) theory, with some discrepancies remaining near the microphase separation transition (MST) where the system is weakly segregated.[3,4] In addition to the overall, common behavior, the differences among systems can be understood on the basis of architecture and the compositional and conformational asymmetry of the molecules.[5,6] The discrepancies between theory and experiment in weak segregation may be due to fluctuation effects which have not yet been incorporated in NSCF theory.[7]

Blends of copolymers, with solvent, homopolymer, or both, offer a rich field of inquiry. They can be single- or two-phase, and each phase can be disordered with all constituents distributed randomly throughout, or ordered. An ordered phase can correspond to any of the many observed structures, i.e., lamellae, cylinders, spheres ordered on a lattice, or one of the more complex structures. Another possibility is spheres distributed randomly through the phase.

Concentrated solutions of copolymer in nonselective good or Θ solvents and in selective solvent have all been treated using NSCF theory.[8−10] The case of dilute solutions is more complex, where swelling effects need to be included.[11,12] There have also been some NSCF calculations on copolymer/homopolymer blends,[13−18] while other theoretical approaches have been used for weakly segregated systems, i.e., near the copolymer MST.

When small amounts of homopolymer are added to neat copolymer, the added homopolymer can be solubilized within the phase. This has been examined in some detail for A homopolymer added to weakly segregated A−B copolymer lamellae.[19−21] Relatively low molecular weight homopolymer tends to destabilize the microphase and to *reduce* the equilibrium layer thickness. Relatively high molecular weight homopolymer has opposite effects: up to the solubilization limit, it further stabilizes the microphase and causes the layer thickness to *increase*. In fact, when relatively high MW homopolymer is added to copolymer which is homogeneous but near the MST, it can induce ordering; this phenomenon is known as induced microphase separation.[19,20,22]

In ref 21, Banaszak and Whitmore developed a theory of these blends which combined a fourth-order expression for the free energy with a nontrivial model of the density profiles. Comparisons of this type of approach with NSCF theory for neat copolymer suggest that it should be a good approximation as long as $\chi N_C \lesssim 15$, where χ is the Flory interaction parameter and N_C is the copolymer degree of polymerization. With this model, they calculated the effects of added homopolymer on copolymer layers, for different combinations of molecular weights, for systems with χN_C in the range of about 10.5−15. The theoretical results were in qualitative agreement with the available experiments, which were done on more strongly segregated systems:[23−25] Low or high molecular weight homopolymer induces a decrease or increase in layer thickness, respectively; there is a threshold MW at which there is no initial change, and this threshold depends on the MW of the homopolymer relative to the copolymer. However, the predicted value of this threshold did not agree quantitatively with experiment.

In this paper, we examine these kinds of systems using NSCF theory, appropriate to all segregation regimes. We focus, in particular, on when added homopolymer causes an increase or decrease in layer thickness, on the distribution of homopolymer within the domains, and on identifying the underlying physical basis of the phenomena. We examine differences between strong and weak segregation, and make comparisons with available experimental data. It is instructive to consider the limits of large and small homopolymer, and we show how the latter reduces exactly to the dilution approximation in the limit of homopolymer whose length is negligible relative to the copolymer. We

10.1021/ma002080x CCC: $20.00
Published on Web 04/13/2001

identify the minimum number of independent parameters needed to predict a blend's equilibrium behavior. This is an extension of earlier work on neat copolymer.[5] Finally, we point out that the NSCF theory can be used to determine χ parameters, complementing techniques that use other theories to determine them from measurements on the homogeneous phase.

2. Numerical Self-Consistent Field Theory and General Results

Numerical SCF theory is well documented in the literature.[1,26−29] Here, we summarize the theory and what needs to be calculated, identify the minimum number of independent variables needed to fully specify the system, and consider some special cases. We present the general case of A-*b*-B copolymer with H homopolymer and the special case where the homopolymer is the same species as one of the copolymer blocks.

2.1. System. We consider a system of $\tilde{N}_H$ homopolymers of type H, and $\tilde{N}_C$ diblock copolymers of type A-*b*-B, in a total volume V. There are three Flory parameters, χ_{AB}, χ_{AH}, and χ_{BH}, and the system is assumed to be incompressible. Each homopolymer has degree of polymerization, statistical segment length, and pure component number density N_H, b_H and ρ_{0H}. The copolymer has block and total degrees of polymerization N_{CA}, N_{CB}, and $N_C = N_{CA} + N_{CB}$, and it has statistical segment lengths and pure component densities b_A, b_B, ρ_{0A}, and ρ_{0B}.

The overall volume fractions of the copolymer and hompolymer can be expressed

$$\bar{\phi}_C = (\tilde{N}_C N_C)/(\rho_{0C} V) \tag{1}$$

$$\bar{\phi}_H = (\tilde{N}_H N_H)/(\rho_{0H} V) \tag{2}$$

where we have introduced the average copolymer density, ρ_{0C}, by

$$\frac{N_C}{\rho_{0C}} = \frac{N_{CA}}{\rho_{0A}} + \frac{N_{CB}}{\rho_{0B}} \tag{3}$$

In addition to the degrees of polymerization N_κ, it is convenient to introduce effective degrees of polymerization for the homopolymer, copolymer, and each block of the copolymer

$$N_\kappa^{\text{eff}} = \frac{\rho_{0R}}{\rho_{0\kappa}} N_\kappa \tag{4}$$

for κ = H, C, CA, and CB, with ρ_{0R} being the reference density used in defining the χ parameters. Each N_κ^{eff} is the volume of the corresponding molecule or block, in units of ρ_{0R}^{-1}. Each N_κ^{eff} reduces to the corresponding N_κ, if we choose all reference densities equal to ρ_{0R}. (N_C^{eff} was denoted r_C in ref 5.)

It will also become apparent that the volumes of each copolymer block and the homopolymer, relative to the copolymer, are important characteristics of the system. All three of these ratios can be written

$$f_\kappa = \frac{N_\kappa^{\text{eff}}}{N_C^{\text{eff}}} \tag{5}$$

for κ = H, A and B. f_A and $f_B = 1 - f_A$ are the volume fractions of the A and B blocks of the copolymer. The overall volume fractions of A and B copolymer in the system are

$$\bar{\phi}_{C\kappa} = f_\kappa \bar{\phi}_C \tag{6}$$

for κ = A and B.

2.2. Self-Consistent Field Equations. We need to calculate a number of chain propagators and self-consistent fields, from which we obtain the equilibrium structure and its free energy, and the volume fraction profiles for each component. In this paper, we assume the equilibrium structure is lamellar, with layer thickness denoted d. The mathematical problem reduces to one dimension.

We need to calculate one propagator for the homopolymer, $q_H(x,\tau)$. It is periodic

$$q_H(x,\tau) = q_H(x+d,\tau) \tag{7}$$

and satisfies the modified diffusion equation

$$\left[-\frac{{b_H}^2}{6}\frac{\partial^2}{\partial x^2} + \omega_H(x)\right] q_H(x,\tau) = -\frac{\partial}{\partial \tau} q_H(x,\tau) \tag{8}$$

and initial condition

$$q_H(x,0) = 1 \tag{9}$$

The local volume fraction of homopolymer at x, denoted $\phi_H(x)$, is constructed from it via

$$\phi_H(x) = \frac{\bar{\phi}_H d}{N_H Q_H} \int_0^{N_H} q_H(x,\tau) q_H(x, N_H - \tau)\, d\tau \tag{10}$$

where

$$Q_H = \int_0^d q_H(x, N_H)\, dx \tag{11}$$

The field acting on a monomer of type H is

$$\omega_H(x) = \frac{\rho_{OR}}{\rho_{0H}}\left\{\chi_{AH}[\phi_{CA}(x) - \bar{\phi}_{CA}] + \chi_{BH}[\phi_{CB}(x) - \bar{\phi}_{CB}] + \frac{\eta(x)}{\rho_{0R}}\right\} \tag{12}$$

where $\eta(x)$ arises from the incompressibility condition.

We need four propagators for the copolymer, which we denote $q_A(x,\tau)$, $q_B(x,\tau)$, $\tilde{q}_A(x,\tau)$, and $\tilde{q}_B(x,\tau)$. They all satisfy the same diffusion equation and periodicity conditions as $q_H(x,\tau)$, but using the corresponding b_κ and $\omega_\kappa(x)$. The first two satisfy the same initial conditions as $q_H(x,\tau)$, but the other two satisfy

$$\tilde{q}_A(x, 0) = q_B(x, N_{CB}) \tag{13}$$

and

$$\tilde{q}_B(x, 0) = q_A(x, N_{CA}) \tag{14}$$

The local volume fraction of $C\kappa$ is

$$\phi_{C\kappa}(x) = \frac{\bar{\phi}_{C\kappa} d}{N_{C\kappa} Q_C} \int_0^{N_{C\kappa}} q_\kappa(x,\tau) \tilde{q}_\kappa(x, N_{C\kappa} - \tau)\, d\tau \tag{15}$$

where

$$Q_C = \int_0^d q_A(x, N_{CA}) q_B(x, N_{CB})\, dx \tag{16}$$

The fields acting on A and B monomers, $\omega_{CA}(x)$ and $\omega_{CB}(x)$, are obtained from eq 12 by appropriate permutations of CA, CB, and H.

If there were solvent present, then it would be conventional to choose ρ_{OR} as the solvent density, and we could express $\eta(x)$ in terms of $\ln[\phi_S(x)]$. In the present case, we determine $\eta(x)$ implicitly. The requirements that the fields $\omega_\kappa(x)$ and all volume fractions are self-consistent, and that the incompressibility condition is satisfied, are sufficient to specify a solution to the above SCF equations. Once this solution is obtained, we can evaluate the free energy per unit volume for the system, relative to its value for a homogeneous system and in dimensionless units, from

$$\frac{F - F_{hom}}{\rho_{0R} k_B T V} = \frac{1}{d}\int_0^d \Big\{ \chi_{AB}[\phi_{CA}(x)\phi_{CB}(x) - \bar{\phi}_{CA}\bar{\phi}_{CB}] + \chi_{AH}[\phi_{CA}(x)\phi_H(x) - \bar{\phi}_{CA}\bar{\phi}_H] + \chi_{BH}[\phi_{CB}(x)\phi_H(x) - \bar{\phi}_{CB}\bar{\phi}_H] - \frac{\rho_{0A}}{\rho_{0R}}\omega_{CA}(x)\phi_{CA}(x) - \frac{\rho_{0B}}{\rho_{0R}}\omega_{CB}(x)\phi_{CB}(x) - \frac{\rho_{0H}}{\rho_{0R}}\omega_H(x)\phi_H(x) \Big\}\, dx - \frac{\bar{\phi}_C}{N_C^{eff}}\ln\left(\frac{Q_C}{d}\right) - \frac{\bar{\phi}_H}{N_H^{eff}}\ln\left(\frac{Q_H}{d}\right) \tag{17}$$

We carry out the calculation as follows. We define a system by the overall volume fractions of each component, the details of those components, i.e., $\rho_{0\kappa}$, N_κ and b_κ, and the three $\chi_{\kappa\kappa'}$. We then make an initial guess for the layer thickness, and find self-consistent solutions and the free energy for that thickness. We then repeat the calculation for different thicknesses, until we find the one that minimizes the free energy.

In the case that the homopolymer is the same species as one of the copolymer blocks, we can choose it to be the A block, i.e., H = A. There is only one nonzero Flory parameter, $\chi_{AB} = \chi_{BH} = \chi$, and $b_A = b_H$, $\rho_{0A} = \rho_{0H}$ and $\chi_{AH} = 0$. The propagators q_H and q_A are the same, although needed for different ranges of τ. The field acting on an A monomer, whether part of a homopolymer or copolymer, is

$$\omega_A(x) = \frac{\rho_{OR}}{\rho_{0A}}\left\{\chi[\phi_{CB}(x) - \bar{\phi}_{CB}] + \frac{\eta(x)}{\rho_{0R}}\right\} \tag{18}$$

The field acting on a B monomer is

$$\omega_B(x) = \frac{\rho_{OR}}{\rho_{0B}}\left\{\chi[\phi_A(x) - \bar{\phi}_A] + \frac{\eta(x)}{\rho_{0R}}\right\} \tag{19}$$

where $\phi_A(x)$ and $\bar{\phi}_A$ have contributions from both copolymer and hompolymer, e.g., $\phi_A(x) = \phi_{CA}(x) + \phi_H(x)$. The free energy, eq 17, simplifies to

$$\frac{F - F_{hom}}{\rho_{0R} k_B T V} = \frac{1}{d}\int_0^d \Big\{ \chi[\phi_A(x)\phi_{CB}(x) - \bar{\phi}_A\bar{\phi}_{CB}] - \frac{\rho_{0A}}{\rho_{0R}}\omega_A(x)\phi_A(x) - \frac{\rho_{0B}}{\rho_{0R}}\omega_{CB}(x)\phi_{CB}(x) \Big\}\, dx - \frac{\bar{\phi}_C}{N_C^{eff}}\ln\left(\frac{Q_C}{d}\right) - \frac{\bar{\phi}_H}{N_H^{eff}}\ln\left(\frac{Q_H}{d}\right) \tag{20}$$

2.3. Factors That Determine the Equilibrium State. As described above, there are a number of factors that specify these systems. In an earlier paper on neat diblocks,[5] we showed that, as long as each possible morphology can be described by a single lattice parameter, e.g., the thickness of the layers, then the equilibrium morphology is controlled by only three parameters. The first of these is χN_C^{eff} where $\chi = \chi_{AB}$ and N_C^{eff} is the effective copolymer degree of polymerization, eq 4. The other two factors are the volume fraction of one of the blocks, f_A or f_B, and the conformational asymmetry, which we can characterize by

$$\epsilon = \frac{\rho_{0B} b_B^{\,2}}{\rho_{0A} b_A^{\,2}} \tag{21}$$

If the monomer volumes are chosen to be equal, this reduces to the ratio of the squares of the statistical segment lengths.

These three parameters determine the equilibrium phase, and the domain size in units of a statistical segment length. To determine this size completely, either b_A or b_B must also be known. Note that, although ρ_{0R} is used to define both the χ parameters and N_C^{eff}, it is not a controlling factor itself; for example, it cancels out in the product χN_C^{eff}.

To identify the minimum number of factors controlling the blends, we first recast the SCF problem in terms of new variables. The first step is to rescale the x and each τ via $x \rightarrow x/d$ and $\tau \rightarrow \tau/N_\kappa$. The next step is to rescale each $\omega_\kappa(x)$ by a factor of $N_C^{eff}\rho_{0\kappa}/\rho_{0R}$, include compensating factors in the SCF equations wherever $\omega_\kappa(x)$ appears, and multiply $\eta(x)$ by $1/\rho_{0R}$. The rescaled potentials become

$$\omega_\kappa(x) = \sum_{\kappa' \neq \kappa} \chi_{\kappa\kappa'} N_C^{eff}[\phi_\kappa(x) - \bar{\phi}_\kappa] + \eta(x) \tag{22}$$

and the diffusion equation for each component becomes

$$\left[-\beta\epsilon_\kappa\frac{\partial^2}{\partial x^2} + \omega_\kappa(x)\right] q_\kappa(x,\tau) = -\frac{1}{f_\kappa}\frac{\partial}{\partial\tau} q_\kappa(x,\tau) \tag{23}$$

The $q_\kappa(x,\tau)$ still obey the initial condition $q_\kappa(x,0) = 1$, but the $\tilde{q}_\kappa(x,\tau)$ now obey

$$\tilde{q}_A(x,0) = q_B(x,1)$$
$$\tilde{q}_B(x,0) = q_A(x,1) \tag{24}$$

The other constants in eq 23 are

$$\beta \equiv \frac{N_C^{eff}\rho_{0H} b_H^{\,2}}{6\rho_{0R} d^2} \tag{25}$$

and

$$\epsilon_\kappa \equiv \frac{\rho_{0\kappa} b_\kappa^{\,2}}{\rho_{0H} b_H^{\,2}} \tag{26}$$

The local volume fractions, $\phi_\kappa(x)$, are calculated from convolutions of the new q_κ and $\tilde{q}_\kappa$. Equations 10 and 15 are replaced by

$$\phi_H(x) = \frac{\bar{\phi}_H}{Q_H}\int_0^1 q_H(x,\tau) q_H(x, 1-\tau)\, d\tau \tag{27}$$

and

$$\phi_{C\kappa}(x) = f_\kappa \frac{\bar{\phi}_C}{Q_C} \int_0^1 q_\kappa(x,1)\tilde{q}_\kappa(x,1-\tau)\, d\tau \qquad (28)$$

and the free energy, eq 17, becomes

$$\frac{F - F_{hom}}{\rho_{0R} k_B T V} = \frac{1}{N_C^{eff}} \left\{ \int_0^1 dx \{ \sum_{\kappa\kappa'} \chi_{\kappa\kappa'} N_C^{eff} [\phi_\kappa(x)\phi_{\kappa'}(x) - \bar{\phi}_\kappa \bar{\phi}_{\kappa'}] - \sum_\kappa \omega_\kappa(x)\phi_\kappa(x) \} - \bar{\phi}_C \ln Q_C - \frac{\bar{\phi}_H}{f_H} \ln Q_H \right\} \qquad (29)$$

The ϵ_κ are generalizations of the asymmetry parameter for neat copolymer.[5,29] We define them here relative to the homopolymer, and so $\epsilon_H = 1$. The parameter β, defined in eq 25, contains the lattice parameter d. Its equilibrium value is determined by minimizing the free energy. Hence, β is not an independent controlling factor. The minimization of the free energy is not affected by the factor of $1/N_C^{eff}$. Thus, we are left with a total of eight parameters needed to determine the details of the layered structure, including its free energy relative to other possible morphologies: one independent volume fraction, $\bar{\phi}_C$ or $\bar{\phi}_H$; the copolymer composition f_A or f_B; two nontrivial parameters ϵ_κ; three parameters $\chi_{\kappa\kappa'}N_C^{eff}$, and f_H. If an overall length scale is also needed, we need one statistical segment length.

This result is easily generalized to other structures that can be characterized by a single lattice constant. This includes the spherical, cyclindrical, and gyroidal morphologies. The only differences in the formalism are that the partial derivatives with respect to x are replaced with the Laplacian operator ∇^2, and the appropriate lattice constant replaces the layer thickness d in the definition of β. This also implies that these eight parameters determine which morphology has the lowest free energy and is the equilibrium one.

For the special case of H = A, there are only one independent χ parameter and one nontrivial conformational asymmetry parameter. This reduces the set of controlling factors to a total of five, plus one statistical segment length. The five can be chosen as f_A, χN_C^{eff} with $\chi = \chi_{AB}$, one nontrivial parameter $\epsilon = \epsilon_B$, $\bar{\phi}_C$, and f_H. The first three of these are the same as those needed for the pure copolymer; the last two describe the overall copolymer/homopolymer concentration and the relative sizes of the homopolymer and copolymer.

2.4. Small Homopolymer Limit and the Dilution Approximation. Our numerical calculations will be for A-*b*-B/A blends, presented in the context of a given χN_C^{eff} and for different f_H. Physically, $N_H^{eff} = 1$ corresponds to a small molecule, i.e., solvent. In one sense, this is a selective solvent, since $\chi_{AH} = 0$ and $\chi_{BH} = \chi \neq 0$. However, when f_H is very small, $N_C^{eff} = 1/f_H$ is large. For a fixed χN_C^{eff}, this in turn implies that χ is small, and the "selective" solvent becomes nonselective. For example, if $N_C^{eff} = 400$, then $\chi N_C^{eff} = 40$ corresponds to $\chi = 0.1$. For a smaller χN_C^{eff}, or larger N_C^{eff} at fixed χN_C^{eff}, χ is even smaller. These all correspond to solvents which are very good for both blocks.

When f_H is small, the homopolymer (solvent) distribution can be calculated analytically. In the diffusion equation, eq 23, the spatial derivatives can be neglected for the homopolymer. Equation 23 then reduces to

$$\omega_H(x) q_H(x,\tau) = -\frac{1}{f_H} \frac{\partial}{\partial \tau} q_H(x,\tau) \qquad (30)$$

which has solution

$$q_H(x,\tau) = e^{-f_H \omega_H(x)\tau} \qquad (31)$$

Substituting this result into eq 27 then gives

$$\phi_H(x) \propto \bar{\phi}_H e^{-f_H \omega_H(x)} \qquad (32)$$

In the limit of $f_H = 0$, $q_H(x,\tau) = 1$, and $\phi_H(x)$ is constant; i.e., the homopolymer (solvent) is distributed uniformly throughout the system. This is equivalent to the dilution approximation, which is an exact solution of the NSCF equations at finite χN_C^{eff} when $f_H = 0$. In the complementary limit of $\chi = 0$ and finite f_H, e.g., $N_H^{eff} = 1$ and finite N_C^{eff}, the potential has no nonzero interaction terms, but it still has a small contribution, $\eta(x)$, arising from the incompressibility condition. The result is that the homopolymer (solvent) density is the same in both subdomains, but there is a small excess in the A−B interphase region.[8] If we approximate the potential by ignoring the $\eta(x)$, then the result is a uniform solvent distribution. This is the dilution approximation again, which is an approximate solution to the NSCF equations if f_H is finite and $\chi = 0$.

For neat copolymer,[29] NSCF theory predicts

$$d \propto \chi^p (N_C^{eff})^{p+1/2} \qquad (33)$$

The value of p is about $^1/_6$ in strong segregation, and increases to $^1/_2$ as $\chi N_C^{eff} \to 10.5$. In the dilution approximation, the layer thickness scales as

$$d \propto \chi_{eff}^{\ p} (N_C^{eff})^{p+1/2} \qquad (34)$$

where χ_{eff} is the effective A−B interaction parameter, defined by

$$\chi_{eff} = \bar{\phi}_C \chi \qquad (35)$$

In the case when χ and f_H are small but finite, $q_H(x,\tau)$ has a weak spatial dependence, which leads to a small difference in density between the A and B subdomains. To leading order, this difference depends on the product χf_H. A sample case is presented in Figure 1, which shows the volume fraction profiles for a very low f_H system. In ref 8, inhomogeneities in the solvent distribution were found to be greatest for large χN_C and $\bar{\phi}_C \simeq 0.5$.

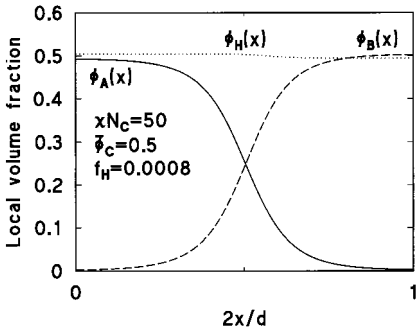

Figure 1. Density profile for a copolymer/homopolymer blend for very small f_H, for the system shown. The copolymer is compositionally and conformationally symmetric.

Hence, for purposes of illustration here, we chose $\chi N_C = 50$, a relatively strongly segregated system, and $\bar{\phi}_C = 0.5$. Even so, the variations in the solvent density are extremely small, limited to less than 1% throughout the entire unit cell.

2.5. Weak Segregation Theory. For compositionally symmetric copolymers, $f_A = 0.5$, the order−disorder transition is second order in mean field theory. When f_A is near to but different from 0.5, it is weakly first order. In this region, the potentials are small, and the solution to the SCF problem can be expanded as a perturbative series. Hong and Noolandi developed this expansion to fourth-order in the fields $\psi_\kappa(x) = \phi_\kappa(x) - \bar{\phi}_\kappa$, which are the variations of the densities about their average values.[19] They showed that each $\psi_\kappa(x)$ is dominated by a single wavenumber. Early work considered only this dominant wavenumber.[19,20] It does not account for the changes in the domain sizes induced by the addition of homopolymer that are observed experimentally.

The "many-wavenumber approximation" (MWA) combines the fourth-order expression for the free energy with multiple wavenumbers in the Fourier expansion of the $\psi_\kappa(x)$ and the potentials. It was developed and used to examine copolymer/homopolymer blends in ref 21. It predicts changes in layer thickness that are qualitatively in agreement with the effects observed in strong segregation. This approach comprises a weak segregation approximation to the full NSCF theory used in the current paper and described above. It is the basis of the comparisons in section 3.

3. Comparison with Weak Segregation Theory

We begin by examining weakly segregated systems and comparing the NSCF results with those of the weak segregation MWA theory. Figure 3 of ref 21 shows the MWA domain and subdomain thicknesses for compositionally and conformationally symmetric A-*b*-B copolymers, $f_A = 0.5$ and $\epsilon = 1$, with added A homopolymer. The copolymer was weakly segregated, with $\chi N_C = 12$. The homopolymer ranged from very low relative size, $f_H = 0.0025$, up to $f_H = 0.3$, and the overall copolymer volume fraction varied from $\bar{\phi}_C = 1$ to $\bar{\phi}_C = 0.8$. Figures 2 and 3 of this paper redo these calculations using the full NSCF formalism. The very low f_H results were obtained for two cases. The first is $f_H = 0.0025$ as in ref 21. The second is $f_H = 0$, calculated using the dilution approximation which, as noted in section 2.4, is an exact solution in this limit. The results for these two cases are indistinguishable.

Figure 2 shows the layer thickness, d, and the A and B sublayer thicknesses, d_A and d_B, for different values of f_H. When there is no homopolymer in a system, they are, of course, independent of f_H, and the results in each panel converge as $\bar{\phi}_C \to 1$. When homopolymer is added, i.e., as $\bar{\phi}_C$ decreases, the thicknesses generally change and change in nontrivial ways.

Qualitatively, the changes are the same as in the MWA model. When relatively large homopolymer is added, e.g., $f_H = 0.3$, both d and d_A increase. Conversely, when relatively small homopolymer is added, e.g., $f_H \to 0$, both d and d_A decrease. In all cases, the B subdomain thickness, d_B, decreases with added homopolymer.

There are, however, quantitative differences. For the neat copolymer, the NSCF approach gives a layer thickness of $d_0/(N_C^{1/2}b) \simeq 1.40$. This is about 4% less than the MWA prediction of about 1.45 for this case. This very small difference is due to the approximations of MWA theory, and would vanish at $\chi N_C = 10.5$. Other differences appear at finite $\bar{\phi}_H$. In Figure 2a, there is a slight increase in d with added homopolymer when $f_H = 0.2$; in the MWA approximation, there was virtually no change for this case. Similarly, in Figure 2b, we see that for $f_H = 0.1$, d_A increases as $\bar{\phi}_C$ decreases, with a

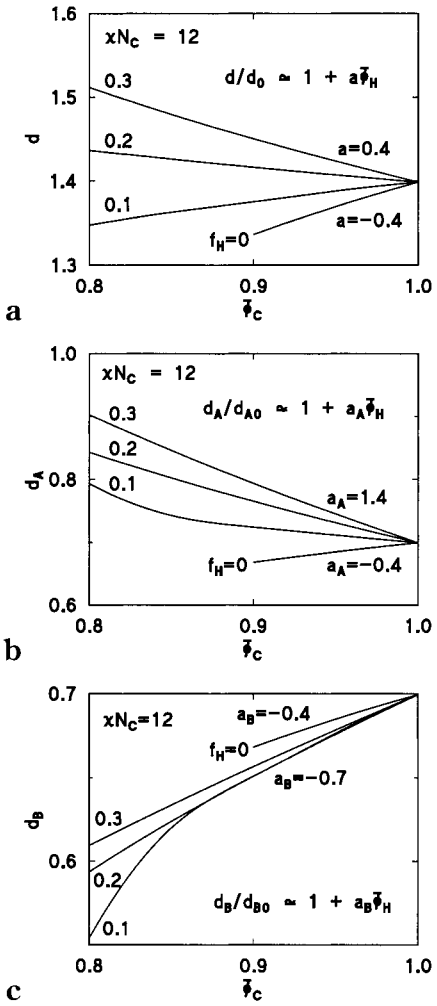

Figure 2. Domain and subdomain thicknesses vs copolymer volume fraction, $\bar{\phi}_C$, calculated using NSCF theory. All thicknesses are expressed in units of $N_C^{1/2}b$. These graphs can be compared with the MWA calculations shown in Figure 3 of ref 21. (a) Domain thickness d, (b) A-subdomain thickness, d_A, and (c) B-subdomain thickness, d_B. To convert to the units of ref 21, multiply by $N_C^{1/2}b = 20b$.

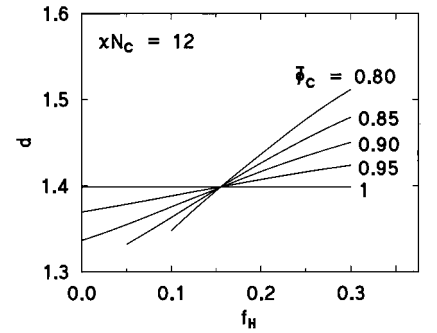

Figure 3. Domain thickness as a function of volume of the homopolymer relative to the copolymer, f_H, using NSCF theory. The units are the same as in Figure 2 of this paper.

slight upward curvature; the corresponding MWA result has a downward curvature in the neighborhood of $\bar{\phi}_C = 0.8$.

The differences can be relatively large, especially for small f_H. As shown in panel a, d approaches d_0 approximately linearly as $\bar{\phi}_C \to 1$. When expressed as a function of $\bar{\phi}_H$, the NSCF results for $f_H = 0$ have a slope of -0.4, i.e.

$$\frac{d}{d_0} \to 1 - 0.4\bar{\phi}_H \tag{36}$$

This slope compares with the value of -1.0 in the MWA result. The NSCF results for d_B, shown in Figure 2c, approach $\bar{\phi}_C = 1$ with a narrower range of slopes than in the MWA results. They also have more downwards curvature near $\bar{\phi}_C = 0.8$ even, as noted above, curving down instead of up for $f_H = 0.1$. Finally, the NSCF values for d_B for small f_H lie above all the other ones, which was not the case for the MWA calculations.

Equation 36 can be understood from the applicability of the dilution approximation at small f_H. Together, eqs 34 and 35 imply

$$d/d_0 = \bar{\phi}_C{}^p \tag{37}$$

Substituting $\bar{\phi}_C = 1 - \bar{\phi}_H$ and expanding for small $\bar{\phi}_H$, eq 37 becomes

$$d/d_0 \simeq 1 - p\bar{\phi}_H \tag{38}$$

which is the linear dependence on $\bar{\phi}_H$ obtained above. For $\chi N_C = 12$, $p \simeq 0.4$,[29] in full agreement with eq 36. This picture also implies that, as χN_C gets closer to 10.5, the slope should become marginally steeper, $p \to 0.5$, although fluctuation effects might mask this effect in real systems.

Figure 3 presents a complementary perspective, showing d vs f_H for different $\bar{\phi}_C$. At each $\bar{\phi}_C$, d varies approximately linearly with f_H, reduced below d_0 at small f_H and increased above d_0 at large f_H. As in the MWA results, the curves all cross $d = d_0$ near a common point, which is the threshold identified in the Introduction. Banaszak and Whitmore found it to be at about $f_H \simeq {}^1/_5$. In these calculations, we find it to be shifted slightly, to about $f_H \simeq {}^1/_6$ at this χN_C. Looking ahead to section 4.1, we find there that this threshold varies with χN_C and with $\bar{\phi}_C$ and that the NSCF and MWA results are in good agreement when $\chi N_C \to 10.5$ and $\bar{\phi}_C \to 1$.

4. Systematic Results

4.1. Domain Thickness. In this section, we describe the systematic study of the effects of homopolymer on the layer thickness, using compositionally and conformationally symmetric copolymers with $f_A = 0.5$ and $\epsilon = 1$, and ρ_{0R} chosen to be equal to $\rho_{0A} = \rho_{0B}$. With these choices, $N_C^{eff} = N_C$ and $N_H^{eff} = N_H$. Most experimental systems have modest conformational asymmetry ($\epsilon \simeq 1$), which does not have major effects except for the exotic phases like the gyroid phase and near phase boundaries between the ordered phases.[3,5]

The systems examined in the study are listed in Table 1. They range from relatively weak to relatively strong segregation, $\chi N_C = 15-50$, copolymer volume fractions from 0.1 to 1, and f_H from zero to 0.5. It is likely that some of these systems are unstable with respect to macrophase separation, a transition to another microphase, or an unbinding transition.[17] Identifying the stability limits would require additional calculations of the kind that have been done for relatively weakly segregated systems,[18] but which we have not done here.

The results vary smoothly with χN_C; for brevity, we show in Figures 4−6 the dependence of d on f_H and $\bar{\phi}_C$ for three sets, using $\chi N_C = 15$, 30, and 50. There are a

Table 1. Model Systems Used in Systematic Study[a]

variable	value
χN_C	15, 20, 30, 40, 50
$\bar{\phi}_C$	0.1, 0.2, 0.3, 0.4, 0.5, 0.6, 0.7, 0.8, 0.85, 0.9, 0.95, 0.99, 1
f_H	0, 0.0008, 0.002, 0.005, 0.0075, 0.01, 0.015, 0.02, 0.0225, 0.025, 0.03, 0.05, 0.075, 0.1, 0.25, 0.5

[a] Systems were derived from all combinations of these parameters, with the additional choices that $f_A = f_B$ and $\epsilon_\kappa = 1$. The limit $f_H = 0$ is calculated from the dilution approximation, using $\chi_{eff} N_C = \bar{\phi}_C \chi N_C$.[8]

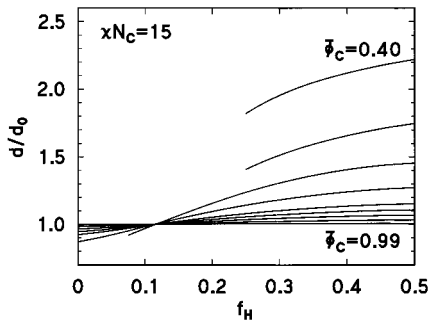

Figure 4. Domain thickness, d, as a function of f_H for $\chi N_C = 15$, relative to the domain thickness for the neat copolymer, d_0. The curves are for $\bar{\phi}_C = 0.4$, 0.5, 0.6, 0.7, 0.8, 0.85, 0.9, 0.95, and 0.99.

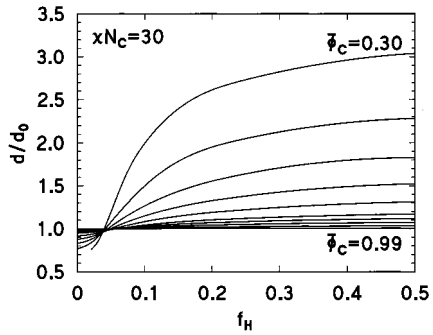

Figure 5. Domain thickness, d, as a function of f_H for χN_C, relative to the domain thickness for the neat copolymer, d_0. The curves are for $\bar{\phi}_C = 0.3$, 0.4, 0.5, 0.6, 0.7, 0.8, 0.85, 0.9, 0.95, and 0.99.

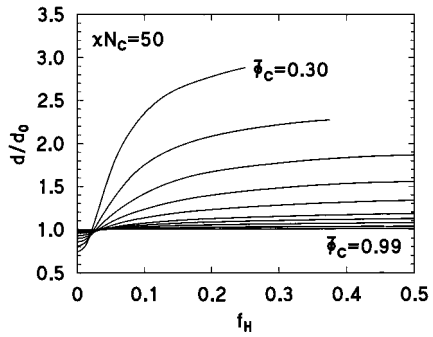

Figure 6. Domain thickness, d, as a function of f_H for $\chi N_C = 50$, relative to the domain thickness for the neat copolymer, d_0. The curves are for $\bar{\phi}_C = 0.3$, 0.4, 0.5, 0.6, 0.7, 0.8, 0.85, 0.9, 0.95, and 0.99.

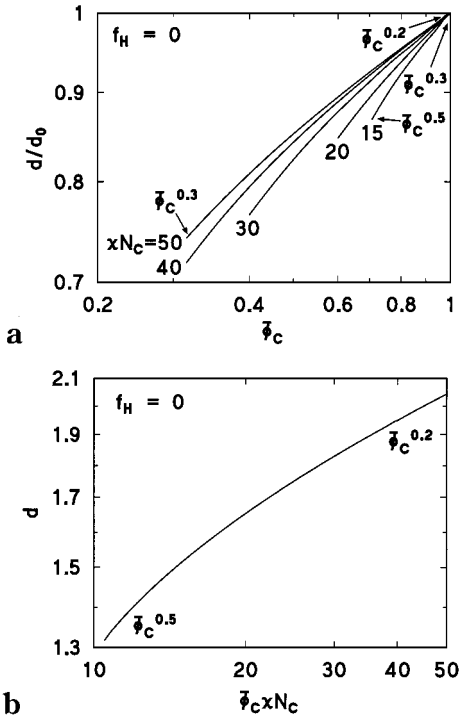

Figure 7. Domain thicknesses for each of the systems in Table 1 for $f_H \to 0$: (a) Layer thickness relative to the neat copolymer case, d/d_0, vs $\bar{\phi}_C$; (b) layer thickness in units of $N_C^{1/2}b$, vs $\bar{\phi}_C\chi N_C$. All results of panel a reduce to this single curve.

number of common features in these results. The most obvious is that, at all segregation strengths, very small homopolymer induces thinner layers, and larger homopolymer induces thicker ones. For any fixed χN_C and $\bar{\phi}_C$, the domain thickness first increases with f_H in an approximately linear fashion. At some intermediate value of f_H, it reaches d_0. As f_H further increases, d continues to increase, though less rapidly. It eventually plateaus at large f_H.

The reduction at small f_H follows directly from the considerations of section 2.4; relatively small homopolymer behaves as a good, nonselective solvent. Hence, we expect $d/d_0 = \bar{\phi}_C^p$ at $f_H = 0$ for all these cases. Figure 7a shows our NSCF results for d/d_0 for χN_C ranging from 15 to 50. For $\chi N_C = 15$, the values of $\chi_{eff}N_C$ range from 15 at $\bar{\phi}_C = 1$ down to 10.5 at $\bar{\phi}_C = 0.7$, which is the MST, and the thickness scales as expected, with effective values of p varying from about 0.3 up to 0.5 at the MST. For stronger segregation, e.g., $\chi N_C = 50$, $\chi_{eff}N_C$ varies from 50 at $\bar{\phi}_C = 1$ down to 15; the power is $p = 0.2$ at $\bar{\phi}_C = 1$ and increases to 0.3 at $\bar{\phi}_C = 0.3$. Note that $p = 0.3$ when $\chi_{eff}N_C = 15$ in both these examples. In Figure 7b, all these results are plotted again, but this time as a function of the $\chi_{eff}N_C$. They all fall on a single curve that corresponds to an approximate power law, with $p \simeq 0.2$ in medium to strong segregation, rising to 0.5 at the MST.

The next figure, Figure 8, shows d/d_0 for a high f_H case, $f_H = 0.5$. In contrast with the low f_H limit, these homopolymers induce a thicker layer, so d/d_0 is a decreasing function of $\bar{\phi}_C$. These results for all five values of χN_C fall very close to a single curve when plotted against $\bar{\phi}_C$. This curve can be expressed approximately as a power law. At high $\bar{\phi}_C$, the power is about $-2/3$, but it quickly shifts to -1.

The increase in d with f_H and its eventual plateauing can be understood on the basis of simple energetic and

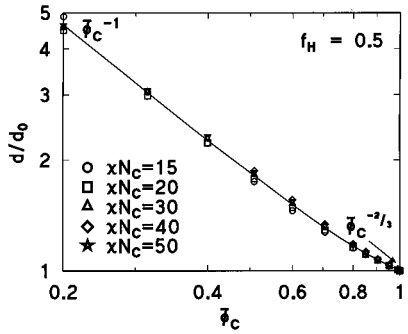

Figure 8. Domain thickness relative to the neat copolymer case, d/d_0, as a function of copolymer volume fraction, $\bar{\phi}_C$, for $f_H = 0.5$.

geometrical arguments. As the size of a homopolymer molecule increases, the energetic cost of its being within the B subdomain or the A−B interphase grows proportionately. Accordingly, for a given set of overall volume fractions, the proportion of homopolymer within the unfavorable subdomain decreases, and it is expelled to the favorable subdomain. Eventually, it will be completely localized within the A-domain. At that point, the thickness d_B becomes independent of the homopolymer characteristics, including f_H. Since we then have the geometric constraint

$$\frac{d_A}{d_B} = \frac{\bar{\phi}_A}{\bar{\phi}_B} = \frac{\bar{\phi}_{CA} + \bar{\phi}_H}{\bar{\phi}_{CB}} \tag{39}$$

it follows that d itself is independent of f_H. The formation of the plateaus in Figures 4−6 corresponds to the complete partitioning of the homopolymer to the A subdomains.

This physical picture is illustrated by the density profiles shown in Figure 9. This is for $\chi N_C = 30$, $\bar{\phi}_C = 0.8$ and $f_H = 0.5$. This system correponds to the right hand end of the fifth lowest curve of Figure 5, where d is almost independent of f_H. We can see in Figure 9 that the homopolymer is indeed completely expelled from the B subdomain and almost completely expelled from the interphase region. The profiles here are very different from those of a very low f_H system, such as Figure 1.

We can carry the argument further to understand the approximate limiting values of d/d_0 at high f_H. Using $d = d_A + d_B$ and $\bar{\phi}_C + \bar{\phi}_H = 1$, eq 39 implies

$$d = \frac{d_B}{f_B\bar{\phi}_C} \tag{40}$$

The d_B appearing here is the thickness of the B-subdomain when all the homopolymer is expelled. Figure 9 suggests that, when the homopolymer is expelled from the interphase, it tends to localize near the center of the A-subdomain. As a result, the interphase is very similar to that for a neat copolymer system. Hence, d_B will be very similar to the corresponding value for the neat copolymer, i.e., $d_B \simeq f_B d_0$. Substituting this into eq 40 yields

$$\frac{d}{d_0} \simeq \frac{1}{\bar{\phi}_C} \tag{41}$$

This equation represents a universal, albeit approximate, explanation of the high f_H limit of all systems, although it must be borne in mind that actually reaching this limit in a real system may be pre-empted by a transition to another phase. It describes the plateau regions of Figures 4−6, and the results of Figure 8. For example, it predicts $d/d_0 \simeq 5$ at $\bar{\phi}_C = 0.2$, as compared with the actual value of 4.6 from Figure 8. This agreement supports the underlying physical picture of expulsion of homopolymer from the unfavorable subdomain and interface for the plateau regions.

With the two extremal cases considered, we turn to intermediate f_H and the thresholds where the domain thickness is equal to the thickness for the neat copolymer, $d = d_0$. From Figures 4−6, we see that there is not a single threshold value of f_H, but that it varies with both χN_C and $\bar{\phi}_C$. Figure 10a shows the thresholds, $f_{H,thresh}$, as functions of $\bar{\phi}_C$ for each χN_C. The largest $f_{H,thresh}$ shown is about 0.13, and it occurs in weak segregation and $\bar{\phi}_C \rightarrow 1$. As the segregation strengthens, *i.e.* χN_C increases, $f_{H,thresh}$ decreases, all the way down to about $f_{H,thresh} = 0.02$ at $\chi N_C = 120$, which is a reduction of about a factor of 6. As well, for each χN_C, the threshold decreases with decreasing $\bar{\phi}_C$.

These dependences are consistent with the physical picture. If the homopolymer penetrates into both subdomains, the copolymer interactions are screened and the layer thickness decreases. When it is effectively completely expelled from the interphase, the layer thickness increases. The threshold occurs when these effects balance. If the amount of homopolymer is small, then a large proportion of it will be soluble in the unfavorable subdomain, and it will be relatively difficult to expel it all from the interphase. Hence relatively high f_H will be needed to reach the threshold; this implies that $f_{H,thresh}$ will increase with decreasing homopolymer content, i.e., increasing $\bar{\phi}_C$. At a given $\bar{\phi}_C$, the segregating strength increases with χN_C, so the homopolymer will be more readily expelled with increasing χN_C ; this implies that $f_{H,thresh}$ will decrease with increasing χN_C. All of this is consistent with the numerical results.

Figure 10b captures these dependences in a simple form. It shows the same values used in Figure 10a, but converted to χN_H by multiplying by χN_C. With a few exceptions, all the points fall very close to a single line, as shown. The points farthest from this line are all at $\chi N_C \bar{\phi}_C \leq 10.5$. The line shown is the line of best fit to all points except the seven for which $\chi N_C \bar{\phi}_C \leq 10.5$. It is described by

$$\chi N_{H,thresh} = 1.39\bar{\phi}_C + 0.68 \tag{42}$$

Expressed this way, the threshold homopolymer size, $N_{H,thresh}$, appears to be a simple function of $\bar{\phi}_C$ and χ^{-1}, there is still an implicit dependence on χN_C because it needs to be large enough that there is a microphase to begin with. A complementary interpretation comes from dividing each side by χN_C, converting it to

$$f_{H,thresh} = \frac{1}{\chi N_C}(1.39\bar{\phi}_C + 0.68) \tag{43}$$

which explicitly indicates an inverse dependence on the copolymer segregation regime, χN_C, and the linear increase with $\bar{\phi}_C$. This picture is consistent with our earlier identification of χN_C, $\bar{\phi}_C$, and f_H as factors determining the equilibrium state.

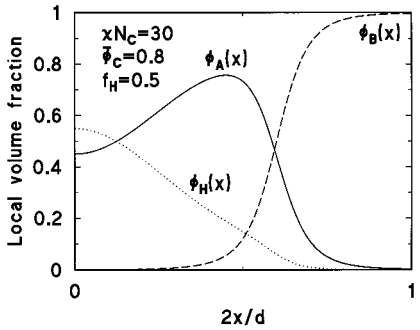

Figure 9. Density profiles for a typical copolymer/homopolymer blend at high f_H. In this example, $\chi N_C = 30$, $\bar{\phi}_C = 0.8$, and $f_H = 0.5$.

Equation 43 provides a basis for quantitative comparison with the MWA prediction. For $\bar{\phi}_C = 1$, it gives

$$f_{H,thresh} = \begin{cases} 0.17, & \text{for } \chi N_C = 12 \\ 0.20, & \text{for } \chi N_C = 10.5 \end{cases} \tag{44}$$

as compared with the MWA value of 0.20 for $\chi N_C = 12$.

The threshold, $f_{H,thresh}$, corresponds to the points where each curve on Figures 4−6 cross $d/d_0 = 1$. A related region is where these same curves cross each other, which occurs at d/d_0 marginally less than unity, and f_H less than $f_{H,thresh}$. Table 2 enumerates the nearest-crossing points, $f_{H,cross}$, of these curves. By definition, these points are where, averaged over $\bar{\phi}_C$, the domain thickness is least influenced by variations in concentration. In weak segregation, the points are all close to each other and to $f_{H,thresh}$, and the corresponding d/d_0 are very close to unity. In strong segregation, the points spread out more and move to lower f_H and d/d_0.

The $f_{H,cross}$ values in Table 2 obey a simple scaling relation

$$f_{H,cross} = 4.50(\chi N_C)^{-1.36} \tag{45}$$

with all points agreeing with it to within ±0.003. For $\chi N_C = 10.5$, eq 45 gives $f_{H,cross} = 0.19$, very close to the MST value of 0.20 for $f_{H,thresh}$.

4.2. Subdomain Thicknesses. We have seen how solubilized homopolymer can be partitioned between the A and B subdomains to widely varying degrees and that it can induce thinner or thicker domains, d. We can anticipate that the effects on the subdomain thicknesses, d_A and d_B, can be complex, and we turn to these now. Following common practice, we identify the boundary between the two by the inflection points in the copolymer density distributions. Although not shown, this also corresponds to the region where the copolymer joint distribution is a maximum. In cases where there are more than one inflection point, such as Figure 9, we use the one closest to the center of the B subdomain.

The systematic NSCF results are shown in Figure 11, which shows d_A/d as a function of χN_H or, equivalently, $\chi N_C f_H$. The behavior of d_B is obtained trivially from $d_B/d = 1 - d_A/d$. In all cases, added homopolymer induces an increase in d_A and a decrease in d_B, relative to d. Of course, d_A itself can still decrease or increase depending on the overall behavior of d.

The limiting behavior at small and large χN_H, or small and large f_H, can be understood as follows. Since the

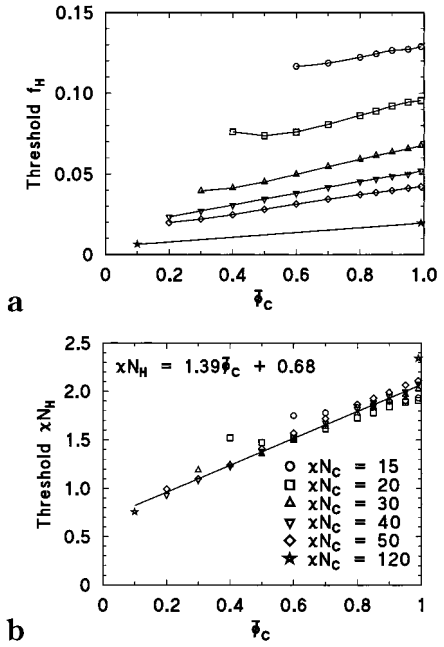

Figure 10. Thresholds for added homopolymer, at which $d = d_0$. Below the threshold, the homopolymer induces a decrease in layer thickness, and above it, the thickness increases. These values were obtained from calculations in Table 1, augmented by two calculations for $\chi N_C = 120$. Key: (a) the threshold, expressed as f_H, as a function of $\bar{\phi}_C$ for each χN_C; (b) same values as in panel a, but converted to χN_H by multiplying by χN_C. The line is the best fit to all the points except those for which $\chi N_C \bar{\phi}_C \leq 10.5$.

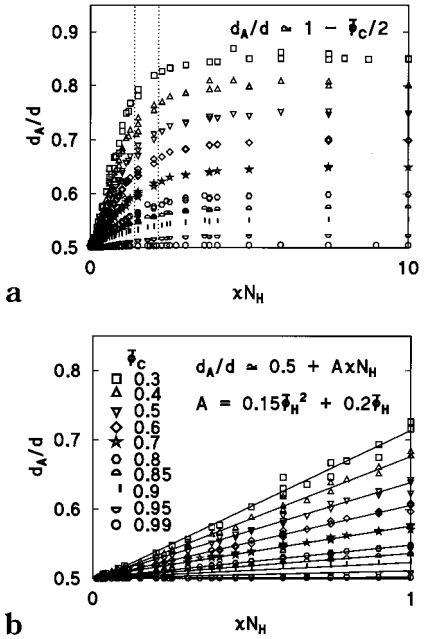

Figure 11. Thickness of the A-subdomain relative to the full layer, d_A/d, vs χN_H. (a) Panel containing the 683 data points from all the converged solutions corresponding to inhomogeneous states for the systems listed in Table 1. For comparison, the range of thresholds where $d = d_0$, as given by eq 42, has been marked. The left-hand dashed vertical line at $\chi N_H = 1.4$ corresponds to the threshold for $\bar{\phi}_C = 0$, and the right-hand line at $\chi N_H = 2.1$ corresponds to the threshold for $\bar{\phi}_C = 1$. (b) Magnification of the results below $\chi N_H = 1$, where the d_A/d dependence on χN_H is approximately linear. In each panel, the horizontal axis is equivalent to $\chi N_C f_H$.

limit $f_H = 0$ corresponds to perfectly nonselective solvent, these homopolymers partition equally between

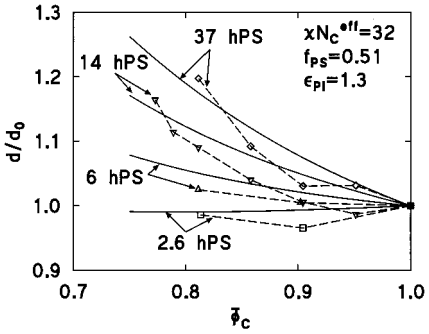

Figure 12. Experimental and NSCF layer thicknesses for four PS-b-PI/PS blends. The copolymer has $N_C^{eff} = 575$. The PS homopolymers, denoted 2.6hPS, 6hPS, 14hPS, and 37hPS, have relative volumes $f_H = 0.05$, 0.12, 0.27, and 0.72, respectively. Thicknesses are expressed relative to the neat copolymer system. Dashed lines with markers indicate experiment.[25] Solid lines indicate NSCF results, which were done using $\chi N_C^{eff} = 32$ and $\epsilon = 1.3$.

the subdomains, and all curves start at $d_A = d_B = d/2$. For small but finite χN_H, there will be more solvent in the A subdomain than the B subdomain, so d_A/d increases. The magnitude of this effect will increase with homopolymer content, so the curves rise more quickly for larger $\bar{\phi}_H$. For small enough χN_H, or equivalently $\chi N_C f_H$, the dependence is linear

$$d_A/d = 0.5 + A\chi N_H \quad \text{if } \chi N_H \lesssim 1$$
$$= 0.5 + A\chi N_C f_H \quad \text{if } \chi N_C f_H \lesssim 1 \tag{46}$$

This is shown is Figure 11b. The slope, A, increases monotonically with ϕ_H

$$A = 0.2\bar{\phi}_H + 0.15\bar{\phi}_H^2 \tag{47}$$

Once the limit when all the homopolymer is in the A subdomain is reached, the relative thicknesses are insensitive to further increases in χN_H or $\chi N_C f_H$, and d/d_0 evolves into a constant whose value depends on $\bar{\phi}_C$. The simple geometric constraints identified in section 4.1 require that $d_A/d = \bar{\phi}_A$ in this limit which, for $f_A = 0.5$, is equivalent to

$$d_A/d \rightarrow 1 - \bar{\phi}_C/2 \tag{48}$$

This limit is reached at $\chi N_H = \chi N_C f_H \simeq 4$. The intermediate region between the dilution limit and this "expulsion" limit occurs over a range which is centered approximately at $\chi N_H \simeq 2$, which corresponds to

$$f_H \simeq \frac{2}{\chi N_C} \tag{49}$$

which is near $f_{H,thresh}$ and $f_{H,cross}$.

5. Experimental Comparisons

We now turn to a comparison of the NSCF predictions with available experimental results. The experiments are the same ones used in ref 21.

The first ones we discuss are the measurements by Winey et al.;[25] their results are shown in Figure 12. They used PS-*b*-PI (polystyrene-*b*-polyisoprene) copolymer blended with PS homopolymer of four different degrees of polymerization. The copolymers were almost perfectly compositionally symmetric with $f_{PS} = 0.51$.

Using $\rho_{0R} = (\rho_{0S}\rho_{0I})^{1/2}$, we obtain $N_C^{eff} = 575$. The neat copolymer is in intermediate segregation, with $\chi N_C^{eff} \simeq 32$.[30] The four homopolymers, which were designated 2.6hPS, 6hPS, 14hPS, and 37hPS, correspond to $f_H = 0.05$, 0.12, 0.27, and 0.72, respectively. Their actual molecular weights are given in ref 25.

Calculating the conformational asymmetry parameter requires the experimental values of the two statistical segment lengths and pure component densities. As discussed in ref 5, literature values vary from $\epsilon = 1$ to 1.3. For this calculation, we use $\epsilon = 1.3$, where the PI block has the longer effective statistical segment length. This value is consistent with moderate asymmetry. As will be seen below, choosing $\epsilon = 1$ or 1.3 has only small effects.

As seen in Figure 12, the measured layer thicknesses appear to be somewhat noisy, but they contain clear trends. High molecular weight homopolymer causes an increase in thickness. At least initially, the lowest MW homopolymer induces a decrease. Otherwise, these homopolymers all induce increases in the thickness, and the rate of increase is an increasing function of N_H or f_H. As $\bar{\phi}_C \rightarrow 1$, the 6hPS appears to correspond approximately to the threshold, which implies $f_{H,thresh} \simeq 0.12$. The results for each homopolymer show upward curvature.

The NSCF results for these systems are also shown on Figure 12. Given the apparent degree of uncertainty in the measurements, and the uncertainty in some of the system parameters needed for the NSCF calculations, the agreement seems quite good, although the experimental results may have slightly more curvature than we find theoretically. The calculated threshold, $f_{H,thresh}$, is between 0.05 and 0.12; eq 43, which is for conformationally symmetric copolymers, gives $f_{H,thresh} \simeq 0.07$ for this degree of segregation.

These NSCF results are qualitatively similar to the MWA ones, but with quantitative differences. In particular, in weak segregation, e.g. $\chi N_C^{eff} \rightarrow 10.5$, the calculated threshold would be $f_{H,thresh} \simeq 0.2$, which is significantly larger than observed or calculated using NSCF theory for this system of $\chi N_C^{eff} \simeq 32$.

The second set of experiments is by Hashimoto et al.,[24] and the results are shown in Figure 13. These experiments also used PS-*b*-PI blended with PS. The molecular weights and polydispersity indices for the copolymer and homopolymers used are given in ref 24. Since, at least up to second order, polydispersity is included in the free energy by using M_w rather than M_n, we consistently use M_w for the copolymer and hompolymers in these calculations. With this choice, the effective degree of polymerization of the copolymer was $N_C^{eff} = 405$. The copolymer was 48% PS by weight, which corresponds to $f_{PS} \simeq 0.45$. They used four different PS homopolymers, denoted S02, S04, S10, and S17, which have relative volumes $f_H = 0.07$, 0.13, 0.28, and 0.47. (They also did some measurements with PI homopolymer, but only in ternary PS-*b*-PI/PS/PI systems which we do not consider in this paper.) With added S02, S04, or S10 homopolymer, the systems remained lamellar at 20% homopolymer by weight, but changed to cylindrical at 50% homopolymer by weight. These weight proportions correspond to $\bar{\phi}_H = 0.19$ and 0.48, respectively. With added S17, the blends remained lamellar all the way to $\bar{\phi}_H = 0.48$.

As shown in Figure 13, when any of the homopolymers were added, the observed layer thickness and PS subdomain thickness increased, with faster increases being caused by the higher molecular weight homopolymer. The PI subdomain thickness always decreased, with faster decreases induced by the lower MW homopolymer. In the case of S17, the presence of 50% homopolymer caused an increase in d_{PI} back toward its value in the neat copolymer system.

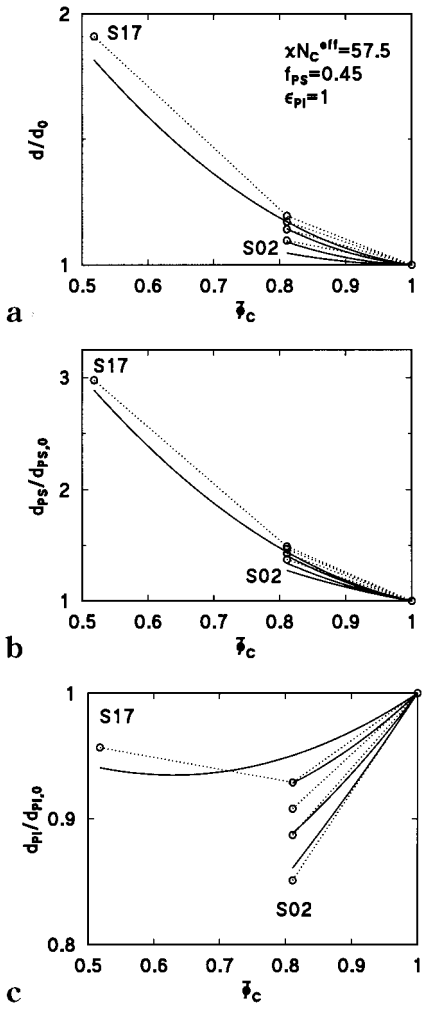

Figure 13. Experimental and NSCF layer and subdomain thicknesses for four PS-b-PI/PS blends. The copolymer has $N_C^{eff} = 405$. The PS homopolymers, denoted S02, S04, S10 and S17, have relative volumes $f_H = 0.07$, 0.13, 0.28, and 0.47, respectively. All thicknesses are expressed relative to the neat copolymer system. Dashed lines with circles indicate experiment.[24] Solid lines indicate NSCF results, which were done using $\chi N_C^{eff} = 57.5$ and $\epsilon = 1.0$. Key: (a) domain thickness, (b) PS subdomain thickness, and (c) PI subdomain thickness.

To make comparisons with experiment, we need to know both the χ and ϵ parameters. Hashimoto et al. found $\chi = 0.035$ for the neat copolymer,[31] corresponding to $\chi N_C^{eff} \simeq 14.2$, which is weak segregation. Using these values, the NSCF calculations produced decreases with added S02, a very slight increase with added S04, and larger increases with the other homopolymers. The S04 was very close to the threshold, indicating $f_{H,thresh} \simeq 0.13$. This is perfectly consistent with our other results in this paper; for example eq 44 gives $f_{H,thresh} \simeq 0.13$ for 20% homopolymer for $\chi N_C^{eff} \simeq 14.2$. It is a typical weak segregation value of the threshold. However, it is significantly smaller than observed in these experiments.

This discrepancy led us to reexamine the choice of χ. We found literature values for χ_{PS-PI} that vary by

Table 2. Values of f_H at Which Domain Thicknesses Exhibit the Least Dependence on $\bar{\phi}_C$[a]

χN_C	f_H at crossing	d/d_0 at crossing
15	0.117	0.999
20	0.075	0.993
30	0.045	0.990
40	0.029	0.970
50	0.023	0.960

[a] These points are calculated from the calculations of Table 1.

Table 3. The Two Sets of Parameters Used to Model the Experimental Systems of Hashimoto et al.,[24] Where, for Each ϵ, the Value of χ Was Found That Reproduced the Observed Layer Thickness for the Neat Copolymer

ϵ	χ	χN_C^{eff}
1.0	0.142	57.5
1.3	0.101	40.8

more than a factor of 2, from 0.035 to 0.086,[10,31] and they often exhibit apparent composition or molecular weight dependences. These values are generally obtained via experiments which are interpreted using theory, which is often a mean field theory even if the experiments are in a range where fluctuation effects can be expected. Some of these experiments also involve the presence of neutral solvent, which might affect results in ways not completely captured by the theories used to interpret them.

For these reasons, we decided that a better test of the blend theory we are presenting here is to find the value of χ which best describes the neat copolymer, and then use this value for all the blends. We did this by finding χ for which the NSCF calculation gave the observed layer thickness for the neat blend, which was $d_0 = 26.7$ nm. There is still one remaining uncertainty, which is the value of ϵ. We used the two limits of the range of values found in the literature, $\epsilon = 1$ and 1.3, and found the required value of χ for each. These values are in Table 3. They are above, but near, the range of values found from other experiments, and they indicate that these systems are in intermediate to strong segregation.

Figure 13 shows our numerical results for the first case, $\epsilon = 1$. The results are qualitatively the same as in the experiments: at 20 wt %, all these homopolymers cause an increase in the layer thickness, d, and the PS sublayer thickness, d_{PS}, and a decrease in d_{PI}; at 50 wt %, the S17 polymer causes a return in d_{PI} toward its original value. The rates of increase and decrease are ordered by the molecular weight of the homopolymer, with the S02 homopolymer causing the slowest increases in d and d_{PS}, and the fastest decrease in d_{PI}. Quantitatively, the theoretical rates of increase are almost, but not quite, as large as the observed ones. For example, 50% S17 leads to an observed increase in d of about 90%, as compared with a theoretical value of about 80%. Both the observed and theoretical values of d_{PS} increase by nearly a factor of 3, and they are in very good agreement with each other. The variations in d_{PI} are smaller, but still in good agreement.

Figure 14 shows our numerical results for the second case, $\epsilon = 1.3$. There are quantitative, but not qualitative differences. Perhaps the most surprising result is that the value of χ needed to produce the neat copolymer d_0 is over 40% larger. Compared with the conformationally symmetric case, Figure 13, the rates of increase in d and d_{PS} are slightly smaller, and the rate of decrease in d_{PI} is slightly greater.

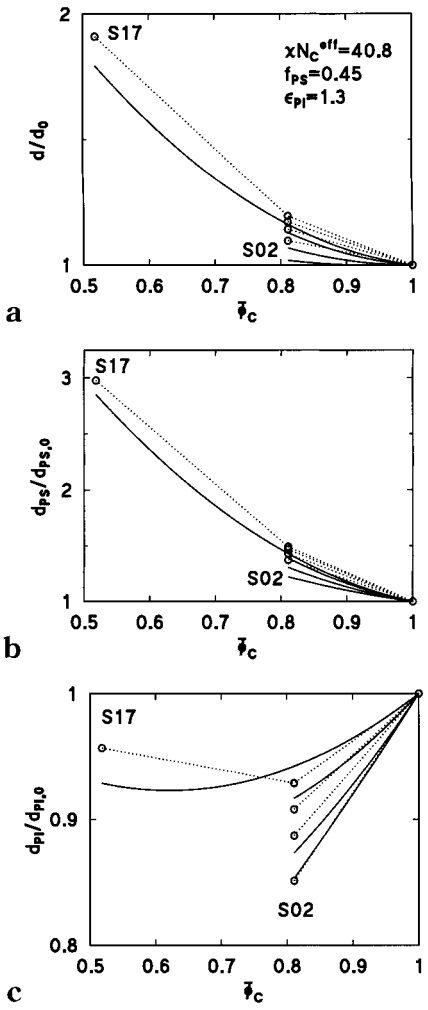

Figure 14. Experimental and NSCF domain and subdomain thicknesses for the same four PS-b-PI/PS blends as in Figure 13. The systems and experimental results are identical to those in Figure 13. The NSCF results were calculated in the same way, except that $\chi N_C^{eff} = 40.8$ and $\epsilon = 1.3$ here. The notation is the same as in Figure 13. Key: (a) domain thickness, (b) PS subdomain thickness, and (c) PI subdomain thickness, all relative to the neat copolymer case.

Both the experiments and the two sets of NSCF results indicate that this system has a threshold value for the increase in d corresponding approximately to S02, which is $f_H \simeq 0.07$, or slightly smaller. Equation 43 gives $f_{H,thresh} \simeq 0.04$ or 0.05 for these degrees of segregation, in good agreement with these full results. This is smaller than $f_{H,thresh}$ for the experiments of Winey et al.,[25] which is consistent with our picture that the neat copolymers in this case are more strongly segregated, i.e., χN_C^{eff} is larger.

6. Concluding Comments

We have examined aspects of homopolymer/diblock copolymer blends using numerical self-consistent field theory. These blends are characterized by a large number of parameters: the degree of polymerization, statistical segment length, and pure component density for the homopolymer and each block of the copolymer, the overall volume fraction of each, and three interaction parameters. Polydispersity would be another factor, although we have not explicitly considered it here.

In section 2.3, we identified the minimum number of parameters needed to predict the equilibrium phase of

these blends. As long as each possible morphology can be characterized by one independent lattice parameter, a total of eight is needed to predict the equilibrium morphology of a general A-*b*-B/H blend: one independent volume fraction, $\bar{\phi}_C$ or $\bar{\phi}_H$; the copolymer composition f_A or f_B; two nontrivial conformational asymmetry parameters ϵ_κ; three parameters $\chi_{\kappa\kappa'}N_C^{eff}$ where $\chi_{\kappa\kappa'}$ are the interaction parameters and N_C^{eff} is an effective copolymer degree of polymerization, and the volume of the homopolymer relative to the copolymer, f_H. If an overall length scale is needed, we also need one statistical segment length. For the special case of H = A, i.e., A-*b*-B/A blends, there are only one nonzero, independent χ parameter, and one nontrivial conformational asymmetry parameter. This reduces the set of controlling factors to a total of five, plus one statistical segment length. The five can be chosen as f_A, χN_C^{eff} with $\chi = \chi_{AB}$, one nontrivial parameter $\epsilon = \epsilon_B$, $\bar{\phi}_C$, and f_H. The first three of these are the same as those needed for the neat copolymer; the last two describe the overall copolymer and homopolymer concentration, and the relative sizes of the homopolymer and copolymer.

The rest of the paper considered the layered structure of A-*b*-B/A blends, and included an analysis of the weak segregation regime with comparisons with an earlier weak segregation theory, comparisons with available experimental results, and a systematic study of systems in varying segregation regimes. We did not attempt to calculate the stability limits relative to other phases. The NSCF and weak segregation theory agree in the limit $\chi N_C \rightarrow 10.5$, but quantitative differences occur even for $\chi N_C \simeq 12$.

An interesting aspect of these systems is that solubilized homopolymer can induce either an increase or decrease in the layer thickness. The weak segregation theory[21] predicted that relatively low molecular weight homopolymer induces a decrease and high molecular weight homopolymer induces an increase. The threshold, i.e., transition between these two effects, occurred around $f_{H,thresh} \simeq {}^1/_5$. This agreed qualitatively, but not quantitatively, with experiment. In this paper, we have found that this threshold value varies with segregation regime and with the composition of the blend to which the homopolymer is being added, i.e., $\bar{\phi}_C$. The variation can be substantial, especially with segregation regime since $f_{H,thresh}$ varies inversely with χN_C: For homopolymer added to neat copolymer, $f_{H,thresh}$ ranges from about 0.2 in very weak segregation down to 0.02 in very strongly segregated systems with $\chi N_C = 100$. For a given χN_C, $f_{H,thresh}$ decreases with increasing homopolymer content, $\bar{\phi}_H$. All these results are succinctly summarized in eq 43.

The results can be interpreted in terms of the controlling factors identified above, and a physical picture. For very small f_H, the homopolymer is much smaller than the copolymer, and behaves much like a solvent. In fact, in the limit of $f_H \rightarrow 0$ and finite χN_C, the effects of the homopolymer can be described exactly by the dilution approximation with the homopolymer playing the role of a nonselective solvent. Entropy drives this homopolymer into both subdomains, which is uniformly distributed in this limit. The copolymer interactions are screened, and the layer thickness decreases. As f_H increases, the balance between the entropic driving forces and the energetic homopolymer-copolymer repulsion changes, and the homopolymer begins to be expelled from the unfavorable subdomain and, eventually, from the AB interphase region. When a large enough fraction of the homopolymer is expelled, the layer thickness increases. When all the homopolymer is expelled from the unfavorable domain and is localized to the interior of the compatible domain, the AB interphase contains only copolymer. In this limit, the unfavorable subdomain thickness is very nearly the same as it would be for neat copolymer. The thickness of the other domain and the overall layer thickness are then simply related by geometric effects.

To relate this physical picture to the controlling parameters, we note first that one characteristic, f_H, is the ratio of the homopolymer and copolymer sizes. Small f_H means that the homopolymer is small on the scale of the copolymer, which is a reasonable criterion for the meaning of "small" for a homopolymer blended with copolymer. The threshold value, $f_{H,thresh}$, reflects when this homopolymer is effectively expelled from the unfavorable domain. If the overall concentration of homopolymer or its molecular weight is small, then a relatively large fraction of it will be soluble in the unfavorable subdomain. This fraction will decrease if the size of the homopolymer, the overall homopolymer volume fraction, or the segregation regime increases. Conversely, for a given fraction of homopolymer to be expelled, its relative size, f_H, will decrease with increasing $\bar{\phi}_H$ or, equivalently, increase with increasing $\bar{\phi}_C$, and decrease with χN_C, as indicated in eq 43.

A complementary physical perspective is afforded by eq 42, which gives the threshold $N_{H,thresh}$ in terms of $\bar{\phi}_C$ and χ, without explicit reference to N_C. Mathematically, this is trivially related to eq 43 by multiplying each side by χN_C. It indicates that the homopolymer is effectively expelled from the subdomain if the energetic driving force per molecule, proportional to χN_H, is sufficiently large. It was noted that there is still an implicit dependence on χN_C.

The predictions of the NSCF theory presented here agree well with the available experiments, if the χ parameter is chosen appropriately. The issues were brought into focus through the comparisons of our results with the experiments of Hashimoto et al. on PS-*b*-PI/PS blends. Available literature values for χ_{PS-PI} vary, but we find that using any of them in the NSCF calculations gives a consistent picture of a too-weakly segregated system with a neat copolymer layer spacing, d_0, which is smaller than is observed, and a threshold value, $f_{H,thresh}$, which is larger than observed. If, however, we choose a larger value of χ_{PS-PI} by requiring that d_0 be given correctly, then $f_{H,thresh}$ also agrees with experiment and NSCF theory gives a consistent picture of a more strongly segregated system.

Determining a χ parameter in this way is similar in spirit to other determinations of it: an experimental measurement is interpreted using a theory to extract its apparent value. In this case, we are in a regime where the effects of fluctuations and solvent on the layer thickness should be nonexistent or negligible. Our resulting values of χ and other predictions for this system are amenable to experimental test. They predict density profiles for each copolymer block which are typical of intermediate to strong segregation. Measurements of such profiles, or of the width of the A−B interphase, should be able to distinguish between these profiles and weak segregation profiles that would be expected for small values of χ although, quantitatively, the interphase may also be broadened by capillary

waves which are not accounted for in the NSCF approach.

Acknowledgment. We thank Drs. B. Bergersen, K. Winey, and M. Winnik and Mr. J. Spiro for many helpful discussions about copolymer/homopolymer blends. This work was supported in part by the Natural Sciences and Engineering Research Council of Canada.

References and Notes

(1) Whitmore, M. D.; Vavasour, J. D. *Acta Polym.* **1995**, *46*, 341.
(2) Whitmore, M. D. Submitted for publication in *Encyclopedia of Materials: Science and Technology*; Lodge, T. P., Section Ed.; Pergamon Press: Oxford, England.
(3) Matsen, M.; Bates, F. S. *J. Polym. Sci. B* **1997**, *35*, 945.
(4) Bates, F. S.; Fredrickson, G. H. *Phys. Today* **1999**, *52* (2), 32.
(5) Vavasour, J. D.; Whitmore, M. D. *Macromolecules* **1993**, *26*, 7070.
(6) Matsen, M. W.; Schick, M. *Macromolecules* **1994**, *27*, 4014.
(7) Fredrickson, G. H.; Helfand, E. *J. Chem. Phys.* **1987**, *87*, 697.
(8) Whitmore, M. D.; Vavasour, J. D. *Macromolecules* **1992**, *25*, 2041.
(9) Banaszak, M.; Whitmore, M. D. *Macromolecules* **1992**, *25*, 3406.
(10) Lodge, T. P.; Hamersky, M. W.; Hanley, K. J.; Huang, C.-I. *Macromolecules* **1997**, *30*, 6139.
(11) Olvera de la Cruz, M. *J. Chem. Phys.* **1989**, *90*, 1995.
(12) Fredrickson, G. H.; Leibler, L. *Macromolecules* **1989**, *22*, 1238.
(13) Shull, K. R.; Winey, K. I. *Macromolecules* **1992**, *25*, 2637.
(14) Shull, K. R.; Mayes, A. M.; Russell, T. P. *Macromolecules* **1993**, *26*, 3929.
(15) Matsen, M. W. *Phys. Rev. Lett.* **1995**, *74*, 4225.
(16) Matsen, M. W. *Macromolecules* **1995**, *28*, 5765.
(17) Janert, P. K.; Schick, M. *Phys. Rev. E.* **1996**, *54*, R33.
(18) Janert, P. K.; Schick, M. *Macromolecules* **1998**, *31*, 1109.
(19) Hong, K. M.; Noolandi, J. *Macromolecules* **1983**, *16*, 1083.
(20) Whitmore, M. D.; Noolandi, J. *Macromolecules* **1985**, *18*, 2486.
(21) Banaszak, M.; Whitmore, M. D. *Macromolecules* **1992**, *25*, 2757.
(22) Cohen, R. E.; Torradas, J. M. *Macromolecules* **1984**, *17*, 1101.
(23) Quan, X.; Gancarz, I.; Koberstein, J. T.; Wignall, G. D. *Macromolecules* **1987**, *20*, 1434.
(24) Hashimoto, T.; Tanaka, T.; Hasegawa, H. *Macromolecules* **1990**, *23*, 4378.
(25) Winey, K. I.; Thomas, E. L.; Fetters, L. J. *Macromolecules* **1991**, *24*, 6182.
(26) Matsen, M. W.; Schick, M. *Phys. Rev. Lett.* **1994**, *16*, 2660.
(27) Matsen, M. W.; Schick, M. *Macromolecules* **1994**, *27*, 6761.
(28) Matsen, M. W.; Schick, M. *Macromolecules* **1994**, *27*, 7157.
(29) Vavasour, J. D.; Whitmore, M. D. *Macromolecules* **1992**, *25*, 5477.
(30) Winey, K. Ph.D. Thesis, University of Massachusetts.
(31) Tanaka, H.; Hashimoto, T. *Macromolecules* **1991**, *24*, 5398.

MA002080X